# BEST AVAILABLE IMAGES

Defective images within this document are accurate representations of the original documents submitted by the applicant.

Defects in the images may include (but are not limited to):

- BLACK BORDERS
- TEXT CUT OFF AT TOP, BOTTOM OR SIDES
- FADED TEXT
- ILLEGIBLE TEXT
- SKEWED/SLANTED IMAGES
- COLORED PHOTOS
- BLACK OR VERY BLACK AND WHITE DARK PHOTOS
- GRAY SCALE DOCUMENTS

## IMAGES ARE BEST AVAILABLE COPY.

**As rescanning documents *will not* correct images, please do not report the images to the Image Problem Mailbox.**


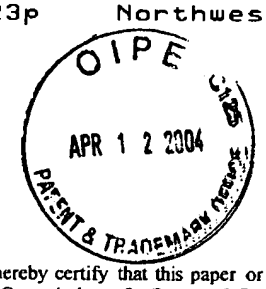


**PATENT**

I hereby certify that this paper or fee is being deposited with sufficient postage as Express Mail No. EV 207284903 US addressed to: Commissioner for Patents, P.O. Box 1450, Alexandria, VA 22313-1450, on April 12, 2004.

Dated: April 12, 2004 BY: Rodney D. DeKruif

Rodney D. DeKruif

IN THE UNITED STATES PATENT AND TRADEMARK OFFICE

| | | |
|---|---|---|
| In re application of : | Barron et al. | ) |
| Serial No: | 09/788,803 | ) |
| | | ) Attorney Docket No. 6374 |
| Filed: | February 16, 2001 | ) |
| For: | POLYPEPTIDE PULMONARY SURFACTANTS | ) |

Commissioner for Patents
P.O. Box 1450
Alexandria, VA 22313-1450

DECLARATION SUPPORTING ENABLEMENT

I, Annelise E. Barron, declare as follows:

1. I am a tenured professor in the Department of Chemical and Biological Engineering, Northwestern University.

2. I am a co-inventor with respect to the above-identified patent application ("the Application") and offer this declaration in support of the specification of the Application enabling both mimics of surfactant protein C (SP-C) and mimics of surfactant protein B (SP-B).

3. I reviewed the pending Office Action and respectfully disagree with the Examiner's conclusions regarding the Nilsson reference. While natural SP-B

has a complex structure and is difficult to synthesize, a short segment from the N-terminus, SP-$B_{1-25}$, has been extensively investigated in the art as a simple mimic for the entire protein. Together with my co-workers and consistent with procedures described in the Application, I synthesized a 25-residue peptide containing the sequence of SP-$B_{1-25}$ with cysteine-alanine substitutions at positions 8 and 11 to prevent unwanted disulfide linkages. This partial sequence was previously shown in the art, as early as 1991, to retain the function of the natural surfactant. Reference is made to endnotes 13-16 of Exhibit A, attached hereto and incorporated herein by reference in its entirety. Exhibit A, a manuscript entitled, "Simple, Helical Peptoid Analogues of Lung Surfactant Protein B", will soon be submitted to *Chemistry and Biology* for publication.

4. The manuscript of Exhibit A provides additional experiments showing SP-B mimics of the type claimed in the Application, having requisite helical structure and length. The SP-B mimics were prepared and tested as taught by the Application and supported by the scientific literature.

I hereby declare that all statements made herein of my own knowledge are true and that all statements made on information and belief are believed to be true; and further that these statements were made with the knowledge that willful false statements and the like so made are punishable by fine or imprisonment, or both, under § 1001 of Title 18 of the United States Code, and that such willful false statements may jeopardize the validity of the above-identified application or any patent issued thereon.

Annelise E. Barron

4/12/04
Date

**Simple, helical peptoid analogues of lung surfactant protein B**

Shannon L. Seurynck, James A. Patch, and Annelise E. Barron

*Department of Chemical and Biological Engineering, Northwestern University, 2145 Sheridan Road, Evanston, Illinois 60208*

Correspondence:
Annelise E. Barron
Associate Professor
Northwestern University
Department of Chemical and Biological Engineering
2145 Sheridan Road
Evanston, IL 60208
(847) 491-2778 (t)
(847) 491-3728 (f)
a-barron@northwestern.edu

**Running Title:** Peptoid analogues of lung surfactant protein B

Exhibit A

## Summary

**There is a clinical need for a biomimetic lung surfactant replacement that contains functional mimics of the hydrophobic, helical lung surfactant proteins B and C. We have designed, synthesized, and characterized simple, non-natural mimics of the N-terminal segment of SP-B (SP-$B_{1-25}$) based on poly-*N*-substituted glycines, or peptoids, which are protease-resistant and able to adopt stable helical secondary structure. Our SP-B peptoid mimics exhibit varying extents of helicity, and have a patterning of hydrophobic and polar residues similar to SP-$B_{1-25}$. Pulsating bubble surfactometry, Langmuir-Wilhelmy surface balance experiments, and fluorescence microscopy images all indicate that lipid/SP-B peptoid films exhibit surface activities similar to that of lipid/SP-$B_{1-25}$ films. With further study and optimization, these novel lung surfactant replacement formulations may have therapeutic applicability for the treatment of respiratory distress syndrome.**

## Introduction

Lung surfactant (LS) is a mixture of lipids and proteins that lines the air/liquid interface of the alveoli. The main function of LS is to reduce and regulate the surface tension within the alveolar network, thereby decreasing the overall work of breathing [1]. Respiratory distress syndrome (RDS), caused by a lack of functional LS, occurs in infants born prior to 32 weeks gestation that are not yet able to secrete LS [1]. Exogenous surfactant replacement therapy (SRT) is commonly used to treat RDS in infants, and has greatly decreased the mortality rate [1]. SRT involves the instillation of animal-derived, or natural, LS replacements into the lung in several doses, however these surfactants are expensive and pose the risk of infection or immune response [2]. Synthetic surfactants, which contain lipids and spreading agents, have been investigated, but generally do not have good *in vivo* efficacy or *in vitro* biophysical activity as compared to natural surfactants [3-5]. Therefore, there is a need for an entirely biomimetic LS replacement that is inexpensive, safe, and bio-available.

In order to develop a functional LS replacement, we must have a thorough understanding of the components of LS and their individual functions. The essential properties for a functional LS replacement are: (i) rapid adsorption to the air/liquid interface, (ii) the ability to respread upon multiple compressions and expansions, and (iii) the ability to reach near zero surface tension at compression [6]. The main lipid component of LS, dipalmitoylphosphatidylcholine (DPPC), has been shown to reach near zero surface tensions upon compression *in vitro*, however is very slow to adsorb to the interface and has poor respreadability [6]. Mixtures of DPPC and acidic phospholipids, such as palmitoyloleoylphosphatidylglycerol (POPG), or other lipids, such as palmitic acid (PA), have been shown to have a higher rate of adsorption and better respreadability, however the minimum surface tension is also increased [7]. Addition of small

amounts of the hydrophobic lung surfactant proteins B and/or C (SP-B and SP-C) to lipid mixtures has been shown to decrease the adsorption rate and induce respreadability while maintaining the low surface tension on compression. [1, 3, 6, 8]

SP-B is a 79 amino acid amphipathic protein with predominantly helical structure. It contains 7 cysteine residues, which form 3 intramolecular and 1 intermolecular disulfide bonds, leading to the formation of a dimer. SP-B is thought to be involved in organization and fluidization of the lipid layer [9], but its specific roles are unknown. Interestingly, it has been shown that SP-B knockout mice are not viable, leading us to believe that SP-B does play an essential role in LS function [10-12]. While mimicking the entire SP-B protein may seem like a daunting task, a small segment from the N-terminus, SP-$B_{1-25}$, has been shown to retain the function of the full length synthetic peptide both *in vitro* and *in vivo* [13-17]. Conformational mapping by FTIR has been performed on SP-$B_{1-25}$ and revealed that residues 1-7 form a hydrophobic, flexible β-sheet, residues 11-21 form an α-helix, and residues 22-25 have a random conformation [18]. More recently, NMR of SP-$B_{11-25}$ has been performed, revealing 35% helicity at 25°C, with the helix containing both cationic and non-polar faces [19]. We have developed mimics of the N-terminal segment of SP-B using poly-*N*-substituted glycines, or peptoids.

There are many families of molecules being investigated as protein mimics for therapeutic purposes. One such family is peptoids which have a similar backbone to peptides with the side chain appended to the amide nitrogen rather than the α-carbon. This change in the backbone structure renders the molecule protease resistant due to the lack of available hydrogen bond donors [20]. The peptoid backbone is also achiral, however stable, helical secondary structure can be induced through the inclusion of chiral side chains [21, 22]. NMR of a peptoid

5-mer homooligomer with chiral side chains revealed poly-proline type I-like helices, with cis-amide bonds, a helical pitch of 6Å, and 3 monomers per turn [23]. Peptoid helices are stable and robust, showing no denaturation up to 75°C in 8 M urea [24]. Studies of heterooligmeric peptoids reveal that helices are most stable if they contain: (i) at least half α-chiral side chains, (ii) an aromatic, α-chiral face, and (iii) a C-terminal aromatic, α-chiral side chain [25]. Peptoids are ideal for mimicry of helical proteins for therapeutic application due to ease of synthesis, ability to form stable helices, and protease resistance.

We have designed and synthesized several simple, helical peptoids with a patterning of cationic and non-polar residues similar to SP-$B_{1-25}$. The surface activity of the peptoid mimics was investigated as compared to an SP-$B_{1-25}$ peptide using the Langmuir-Wilhelmy surface balance, fluorescence microscopy, and pulsating bubble surfactometer. These results revealed that the simple peptoid mimics are able to capture many of the features of the SP-$B_{1-25}$ peptide. The biomimetic LS replacement that we have developed shows promise for treatment of RDS.

## Results and Discussion

### *Design of mimics*

SP-B is known to be essential to proper LS function, however it is difficult to synthesize due to its relatively large size and complexity. Therefore, small segments of this protein have been investigated for their *in vitro* surface activity and *in vivo* efficacy. A segment from the N-terminus, SP-$B_{1-25}$, has been extensively investigated and shows promise as a simple mimic for the entire protein [13-16]. As a positive control for our peptoid mimics, we have synthesized a 25 residue peptide containing the sequence of SP-$B_{1-25}$ with cysteine  alanine substitutions at positions 8 and 11 (Figure 1) to prevent unwanted disulfide linkages. This modified sequence

has previously been shown to retain the function of the original sequence [16]. Final purity was confirmed to be >97% by reversed-phase HPLC and mass was confirmed to be 2864 Da by ESI.

SP-B peptoid mimics were designed to capture 3 main features of this N-terminal segment thought to be important to its function: (i) overall helicity, (ii) overall hydrophobicity, and (iii) cationic and non-polar faces. In order to maintain a stable, helical secondary structure we included the following in both of our mimics: (i) at lease one-half α-chiral side chains, (ii) an α-chiral, aromatic face, and (iii) a C-terminal α-chiral, aromatic side chain [25]. We determined that the proper length of the peptoid, based on 3.6 residues/turn and 5.4 Å/turn for the peptide and 3 monomers/turn and 6 Å/monomer for the peptoid, would be 19 monomers. However, since we include 1/3 achiral side chains, the helix will be slightly looser, so we have designed peptoids 17 monomers in length. In order to create a cationic face, we have placed a lysine side chain (*N*Lys) every third monomer. For peptoid **1**, the remaining 2/3 side chains are *N*-(S)-phenylethyl (*N*spe), which are α-chiral and aromatic, and create very stable helical molecules. We have also designed a peptoid **2** that is more biomimetic in nature, including an α-chiral, aliphatic isoleucine side chain, *N*-(S)-sec-butylamine (*N*ssb), every third monomer, while still maintaining an aromatic face. Finally, we have created an entirely biomimetic peptoid **3** with *N*Lys every third monomer and *N*ssb constituting the remaining 2/3 of the molecule. Since peptoid **3** does not contain any aromatic side chains, it is expected to be less helical and have a polyproline type-I-like CD spectrum. Purity of the peptoids was confirmed to be >97% by reversed-phase HPLC and masses were confirmed by ESI (**1** – 2592 Da, **2** – 2304 Da, **3** – 2016 Da).

*Circular dichroism*

Helicity of the molecules was confirmed using circular dichroism (CD). Figure 2A is a comparison of the CD spectra for SP-$B_{1-25}$ and peptoids **1** and **2** in water at room temperature. Interestingly, we find that SP-B has spectra characteristic of random coil conformation under these conditions. Both peptoid mimics have α-helix like spectra (minima at λ ~202 nm and ~218 nm and a maximum at λ ~189 nm), previously shown to correspond to a polyproline type I-like helix for peptoids [23]. As expected due to the high aromatic content of the molecule, the spectrum for **1** has more intense helical features than that for **2**. The CD spectrum for **3** was that typically seen for random coil conformation (data not shown).

CD was also performed in 1 mM liposomes (DPPC:POPG:PA 68:22:9) to investigate helicity in a lipid environment similar to that of LS (Figure 2B). All molecules had spectra characteristic of helices, however the spectrum for **3** was that typically seen for a polyproline type-I helix (data not shown). This type of spectrum has previously been observed when chiral, aliphatic side chains are used [25]. The spectra for SP-$B_{1-25}$, **1**, and **2** were all similar to that associated with α-helical structure, with minima at λ ~209 nm and 223 nm and a maximum at λ ~193 nm. The spectra have greater intensity and are shifted toward higher wavelength than those observed in water, implying a greater helical content under these conditions. The peptoids **1** and **2** both had a more intense minima at ~220 nm compared to that at ~ 205 nm, corresponding to more stable helical structure [22, 25]. This was not observed in water, indicating that the lipid environment induces helical stability. Similar spectra were observed for all molecules when performed in organic solution (methanol, data not shown).

*Langmuir-Wilhelmy surface balance (LWSB)*

LWSB isotherms for good LS replacements should have an early lift-off (rapid adsorption to interface), high collapse pressure (near 70 mN/m, corresponds to near zero surface

tension), and a plateau around 40-50 mN/m (corresponding to a phase transition or squeeze-out of molecules from the monolayer) [26]. We collected surface pressure-area isotherms for lipids alone, lipids with 2.16 mol% SP-$B_{1-25}$, and lipids with 2.16 mol% of either peptoid **1**, **2**, or **3** at 25°C and 37°C (Figure 3, **3** not shown). Only isotherms for 25°C are shown, however similar trends were observed at 37°C. Lipids alone had a lift-off of ~87 $Å^2$/molecule at 25°C. The lipid/SP-$B_{1-25}$ mixture has an earlier lift-off, ~110 $Å^2$/molecule, and a plateau at ~50 mN/m is present. When either peptoid **1**, **2**, or **3** is included with the lipids, we observe similar isotherms to the lipid/SP-$B_{1-25}$ mixture with lift-offs of ~100 mN/m and plateaus at ~45 mN/m. Interestingly, the plateau for the lipid/peptoid **1** combination is even more dramatic than that seen for the lipid/peptide mixture, similar to that observed for natural LS (REF). We believe this occurs due to the high helicity of the molecule relative to SP-$B_{1-25}$.

*Fluorescence microscopy imaging*

FM in conjunction with LWSB was used to investigate the phase morphology of lipid, lipid/peptide, and lipid/peptoid samples. The samples were spiked with 1 mol% of a Texas Red conjugated lipid, which resides in the more expanded phase. Therefore, in the FM images shown in Figure 4 the lighter regions correspond to the more expanded phase while the darker regions correspond to the more condensed phase. FM images obtained at 37°C for lipids (A and E), lipid/SP-$B_{1-25}$ (B and F), lipid/**1** (C and G), and lipid/**2** (D and H) at 3~0mN/m (A-D) and ~45 mN/m (E-F) are shown in Figure 4. At 30 mN/m the lipids alone have quite large domains that are rather spread out (Figure 4A). With the addition of SP-$B_{1-25}$ to the lipids, there is a decrease in the domain size as well as a more closely packed arrangement (Figure 4B). FM of both lipid/**1** and lipid/**2** mixtures reveal a coexistence of large and small domains, with a packing arrangement intermediate to that of lipids alone and lipid/SP-$B_{1-25}$ (Figure 4C-D). Similar results

are obtained at 45 mN/m with lipids alone having large, rather spaced out domains (Figure 4E), lipid/SP-$B_{1-25}$ have small, closely packed domains (Figure 4F), and lipid/**1** and lipid/**2** have an intermediate domain size and spacing to lipids alone and lipid/SP-$B_{1-25}$ (Figure 4G-H). Overall, our peptoid mimics appear to have phase morphology intermediate to that of lipids alone and lipids with 2.16 mol% SP-$B_{1-25}$.

*Pulsating bubble surfactometry*

Pulsating bubble surfactometry was used to characterize the surface activity of our samples under both static and dynamic conditions. Natural LS would have an adsorption rate on the order of one minute and a hysteresis loop (interfacial area *vs.* surface tension) with a maximum surface tension of ~35 mN/m, a minimum near zero, and rapid adsorption to the interface upon compression [27]. Static adsorption data was collected for lipids alone, lipid/SP-$B_{1-25}$, and lipid/peptoid **1**, **2**, or **3** over 20 minutes at 37°C (Figure 5A, **3** not shown). The equilibrium surface tension for lipids alone was 41 mN/m and took nearly 20 minutes to reach. With added SP-$B_{1-25}$ the surface tension rapidly decreased to 40 mN/m in only 2 minutes and then slowly decreased to an equilibrium surface tension of 30 mN/m. The addition of peptoid **1**, **2**, or **3** to the lipids had a similar effect, with an immediate decrease to 40 mN/m and a gradual decrease to the equilibrium surface tension of 32 mN/m.

Dynamic adsorption data was collected for lipids, lipids/SP-$B_{1-25}$, and lipids/peptoid **1**, **2**, or **3** at 37°C with a pulsation rate of 20 cycles/min. Interfacial area-surface tension hysteresis loops are shown in Figure 5B (**3** not shown). The loop for lipids alone has a very small amount of hysteresis, reaches a minimum surface tension of only 7 mN/m, and has a high maximum surface tension of 57 mN/m. Upon the addition of SP-$B_{1-25}$ to the lipids, there is a decrease in the minimum and maximum surface tensions, to 4 mN/m and 42 mN/m, respectively. There is

also an increase in the hysteresis, indicating faster adsorption upon compression. With the addition of either peptoid **1** or **2**, a minimum surface tension similar to that of the lipid/SP-$B_{1-25}$ mixture is observed, however the maximum surface tension is intermediate to that of lipids alone and the lipid/SP-$B_{1-25}$ mixture (49 mN/m). Interestingly, the hysteresis loops for peptoid 1 and 2 both have an increase in hysteresis compared to the loop for SP-$B_{1-25}$, indicating that the peptoid mimics of SP-B may actually be working better than the peptide segment. The loop for peptoid **3** has hysteresis similar to that of peptoid **2**.

**Significance**

**We have created several simple, helical peptoid mimics of the N-terminal segment of SP-B that are able to retain the function of SP-$B_{1-25}$ peptide. Our peptoid mimics were designed to maintain the helical secondary structure of SP-$B_{1-25}$ as well as have a similar patterning of hydrophobic and cationic side chains. Testing of our SP-B peptoid mimics by LWSB, FM, and PBS reveals that the lipid/peptoid films behave similarly to the of lipid/SP-$B_{1-25}$ films. These simple peptoid analogues will be further investigated in a rat model of respiratory distress syndrome to determine applicability for clinical treatment.**

**This entirely biomimetic formulation would fill a clinical need for a safe, bioavailable, and inexpensive LS replacement for the treatment of respiratory distress syndrome. Some of the many advantages of using peptoids in therapeutic formulations are the ability to form stable helical secondary structure and resist aggregation, resistance to protease degradation, low cost, and relatively simple synthesis. The ability of these simple, helical peptoids to mimic the behavior of the peptide in a lipid environment indicates that**

**peptoids and other biopolymers have potential for broad application in therapeutic formulations that depend on lipid/protein interactions.**


## Acknowledgements

We thank Mark Johnson, Ronald N. Zuckermann, and Nathan J. Brown for their assistance. We acknowledge use of the Keck Biophysics Facility at Northwestern University for CD measurements. We acknowledge support for this work from the National Science Foundation (Grant Nos. BES-9870386 and BES-0101195) and the National Institute of Health (Grant No. 1R01HL67984-01). JAP was supported by an NIH Molecular Biophysics Training Grant (Grant No. 5 T32 GM08382-10).


## Experimental Procedures

*Materials*

Peptide and peptoid synthesis reagents were purchased from Applied Biosystems (Foster City, CA) or Aldrich (Milwaukee, WI). Resins, Fmoc-protected amino acids, and $(t\text{-Boc})_2O$ were purchased from NovaBiochem (San Diego, CA), and primary amines were purchased from Aldrich. Solvents for HPLC were purchased from Fisher Scientific (Pittsburgh, PA). DPPC, POPG, and Texas Red-DHPE were purchased from Avanti Polar Lipids (Alabaster, AL) and PA was purchased from Aldrich. All chemicals were used without further purification.

*Peptide and peptoid synthesis*

$SP\text{-}B_{1\text{-}25}$, with a cys ala substitution to prevent disulfide bond formation, was synthesized by Fmoc chemistry on solid support using an ABI 433A automated peptide synthesizer (Applied Biosystems). Peptoids were also synthesized using the ABI 433A on Rink

amide resin following a submonomer protocol [28], with Boc protection of the *N*Lys side chain [29]. Peptide and peptoid oligomers were cleaved from the resin with a mixture of 95% TFA/water along with necessary protecting group scavengers. Molecules were purified by reversed-phase HPLC using a linear gradient of 20%-95% solvent B in solvent A over min (solvent A is 0.1% TFA in water [v/v] and solvent B is 0.1% TFA in acetonitrile [v/v]). Final purities of the molecules were confirmed to be >97% by analytical reversed-phase HPLC and molecular weights were confirmed by electrospray mass spectrometry (ESI).

*Sample preparation*

DPPC, POPG, and PA were dissolved to a known concentration (~2 mg/ml) in a 3:1 solution of chloroform and methanol. DPPC, POPG, and PA were combined at a ratio of 68:22:9 to a concentration of ~2 mg/ml. This lipid formulation has previously been shown to be a good mimic of the lipid portion of LS [30]. For circular dichroism in liposomes, lipids were dried under nitrogen and dissolved in 4 mM TRIS buffer under sonication at 50°C for ~60 min to a final concentration of 2 mM. For surface activity studies, peptide or peptoid was added to the lipid mixture at 2.16 mol% (corresponding to 10 wt% of SP-$B_{1-25}$), to a final concentration of ~1 mg lipid/ml.

*Circular dichroism*

Circular dichroism (CD) was performed in water, methanol, and a liposome formulation (DPPC:POPG:PA 68:22:9). Peptide and peptoid samples were prepared in water, methanol, or lipids (1 mM) and buffer to a final concentration of ~60 μM. CD was performed on a Jasco J-715 instrument using a cylindrical quartz cuvette (Hellma, Plainview, BY) with a 0.02 cm path length at room temperature. Each spectrum represents the average of 40 accumulations.

*Langmuir-Wilhelmy surface balance (LWSB)*

Our home-built LWSB consists of Langmuir trough fabricated from a solid piece of Teflon and epoxied to a copper plate. Two Teflon barriers are located at opposite ends of the trough and are controlled by a Unislide assembly (Velmex, Bloomfield, NY) with a Silvermax motor (Quicksilver Controls, Covina, CA) to adjust the surface area. Both barriers are spring-loaded against the trough to prevent surfactant leakage up to 72 mN/m. The subphase temperature is measured *via* a thermistor and controlled by twelve thermoelectric couples (Marlow Industries, Dallas, Texas) that are connected in series and located between two copper plates. Continuous surface pressure measurements are obtained by a Wilhemy plate transducer controlled by a feedback loop (R&K, Berlin, Germany). The barrier control, temperature control, and pressure transducer are all interfaced with a computer to record experimental data.

For the experiments, the trough was filled with ~300 ml buffer (150 mM NaCl, 5 mM $CaCl_2$, 10 mM HEPES, pH 6.9) and heated to either 25°C or 37°C. The sample, dissolved in a mixture of 3:1 chloroform and methanol, was spread at the air/liquid interface and allowed to evaporate for 10 min. The barriers were cycled at 30 mm/min.

*Fluorescence Microscopy (FM)*

In order to obtain FM images, a Nikon MM40 compact microscope stand with a 100W mercury lamp (Tokyo, Japan) is used in conjunction with the LWSB to visualize surface morphology of the monolayer. The fluorescence is detected by a Dage-MTI three-chip color camera (Dage-MTI, Michigan City, IN) in conjunction with a generation II intensifier (Fryer, Huntley, IL). Samples were spiked with 1 mol% of a fluorescently labeled lipid, Texas Red-DHPE, for detection. Experiments were performed on a buffered subphase at 37°C with a barrier speed of 2-10 mm/min.

*Pulsating bubble surfactometer (PBS)*

The PBS was used to obtain both static and dynamic adsorption data. Samples were dried using a DNA 120 speedvac (Thermo Electron, Holbrook, NY), forming a pellet. The pellet was dissolved in buffer (150 mM NaCl, 5 mM $CaCl_2$, 10 mM HEPES, pH 6.9) to 1.0 mg/ml, with a final volume of ~ 70 µl. Samples were mixed with a pipette, sonicated with a Fisher Model 60 (Hanover Park, IL) probe sonicator, and then mixed with a pipette again to form a uniform solution. Samples were loaded into a sample chamber with putty placed on the capillary end of the sample chamber, a method previously shown to prevent sample leakage into the capillary [31]. All experiments were performed at 37°C. Static adsorption data was collected for 20 minutes. Dynamic adsorption data was obtained at a frequency of 20 cycles/min for 20 min following static adsorption.

**References**

1. R. H. Notter (2000). Lung Surfactants: Basic Science and Clinical Applications. (New York: Marcel Dekker).

2. B. Robertson, J. Johansson and T. Curstedt (2000). Synthetic surfactants to treat neonatal lung disease. Molecular Medicine Today *6*, 119-124.

3. S. B. Hall, A. R. Venkitaraman, J. A. Whitsett, B. A. Holm and R. H. Notter (1992). Importance of hydrophobic apoproteins as constituents of clinical exogenous surfactants. Annual Review in Respiratory Distress *145*, 24-30.

4. J. J. Cummings, B. A. Holm, M. L. Hudak, B. B. Hudak, W. H. Ferguson and E. A. Egan (1992). A Controlled Clinical Comparison of 4 Different Surfactant Preparations in Surfactant-Deficient Preterm Lambs. American Review of Respiratory Disease *145*, 999-1004.

5. K. Mizuno, M. Ikegami, C. M. Chen, T. Ueda and A. H. Jobe (1995). Surfactant Protein-B Supplementation Improves in-Vivo Function of a Modified Natural Surfactant. Pediatric Research *37*, 271-276.

6. J. Goerke and J. A. Clements (1986). Alevolar surface tension and lung surfactant. In Handbook of Physiology. Sec. 3, The Respiratory System. Vol. 3, Mechanics of Breathing: Part I., A. Fishman, P. Macklem, J. Mead and S. Geiger, editors. (Bethesda, MD: American Physiological Society). pp 247-262.

7. R. Veldhuizen, K. Nag, S. Orgeig and F. Possmayer (1998). The role of lipids in pulmonary surfactant. Biochimica et Biophysica Acta *1408*, 90-108.

8. Z. Wang, S. B. Hall and R. H. Notter (1996). Roles of different hydrophobic constituents in the adsorption of pulmonary surfactant. Journal of Lipid Research *37*, 790-798.

9. J. E. Baatz, B. Elledge and J. A. Whitsett (1990). Surfactant protein SP-B induces ordering at the surface of model membrane bilayers. Biochemistry *29*, 6714-6720.

10. J. C. Clark, S. E. Wert, C. J. Bachurski, M. T. Stahlman, B. R. Stripp, T. E. Weaver and J. A. Whitsett (1995). Targeted Disruption of the Surfactant Protein-B Gene Disrupts Surfactant Homeostasis, Causing Respiratory-Failure in Newborn Mice. Proceedings of the National Academy of Sciences of the United States of America *92*, 7794-7798.

11. S. W. Glasser, M. S. Burhans, T. R. Korfhagen, C.-L. Na, P. D. Sly, G. F. Ross, M. Ikegami and J. A. Whitsett (2001). Altered stability of pulmonary surfactant in SP-C-deficient mice. PNAS *98*, 6366-6371.

12. K. Tokieda, H. S. Iwamoto, C. Bachurski, S. E. Wert, W. M. Hull, K. Ikeda and J. A. Whitsett (1999). Surfactant protein-B-deficient mice are susceptible to hyperoxic lung injury. American Journal of Respiratory Cell and Molecular Biology *21*, 463-472.

13. A. Waring, H. W. Taeusch, R. Bruni, J. Amirkhanian, B. C. R. Fan, R. Stevens and J. Young (1989). Synthetic amphipathic sequences of surfactant protein B mimic several physiochemical and in vivo properties of native pulmonary surfactant proteins. Peptide Research *2*, 308-313.

14. S. D. Revak, T. A. Merritt, M. Hallman, G. Heldt, R. J. Lapolla, K. Hoey, R. A. Houghten and C. G. Cochrane (1991). The Use of Synthetic Peptides in the Formation of Biophysically and Biologically-Active Pulmonary Surfactants. Pediatric Research *29*, 460-465.

15. M. L. Longo, A. M. Bisagno, J. A. N. Zasadzinski, R. Bruni and A. J. Waring (1993). A Function of Lung Surfactant Protein Sp-B. Science *261*, 453-456.

16. R. Bruni, H. W. Taeusch and A. J. Waring (1991). Surfactant protein B: Lipid interactions of synthetic peptides representing the amino-terminal amphipathic domain. Proceedings of the National Academy of Sciences *88*, 7451-7455.

17. J. E. Baatz, V. Sarin, D. R. Absolom, C. Baxter and J. A. Whitsett (1991). Effects of Surfactant-Associated Protein Sp-B Synthetic Analogs on the Structure and Surface-Activity of Model Membrane Bilayers. Chemistry and Physics of Lipids *60*, 163-178.

18. L. M. Gordon, K. Y. C. Lee, M. M. Lipp, J. A. Zasadzinski, F. J. Walther, M. A. Sherman and A. J. Waring (2000). Conformational mapping of the N-terminal segment of surfactant protein B in lipid using C-13-enhanced Fourier transform infrared spectroscopy. Journal of Peptide Research *55*, 330-347.

19. J. W. Kurutz and K. Y. C. Lee (2002). NMR structure of lung surfactant peptide SP-B11-25. Biochemistry *41*, 9627-9636.

20. S. M. Miller, R. J. Simon, S. Ng, R. N. Zuckermann, J. M. Kerr and W. H. Moos (1995). Comparison of the proteolytic susceptibilities of homologous L-amino acid, D-amino acid, and N-substituted glycine peptide and peptoid oligomers. Drug Development Research *35*, 20-32.

21. K. Kirshenbaum, A. E. Barron, R. A. Goldsmith, P. Armand, E. K. Bradley, K. T. V. Truong, K. A. Dill and F. E. Cohen (1998). Sequence-specific polypeptoids: A diverse family of heteropolymers with stable secondary structure. Proceedings of the National Academy of Sciences *95*, 4303-4308.

22. C. W. Wu, T. J. Sanborn, R. N. Zuckermann and A. Barron (2001). Peptoid oligomers with a-chiral, aromatic side chains: Effects of chain length on secondary structure. Journal of the American Chemical Society *123*, 2958-2963.

23. P. Armand, K. Kirshenbaum, R. A. Goldsmith, S. Farr-Jones, A. E. Barron, K. T. V. Truong, K. A. Dill, D. F. Mierke, F. E. Cohen, R. N. Zuckermann and E. K. Bradley (1998). NMR determination fo the major solution conformation of a peptoid pentamer with chiral side chains. Proceedings of the National Academy of Sciences *95*, 4309-4314.

24. T. J. Sanborn, C. W. Wu, R. N. Zuckerman and A. E. Barron (2002). Extreme stability of helices formed by water-soluble poly-N- substituted glycines (polypeptoids) with alpha-chiral side chains. Biopolymers *63*, 12-20.

25. C. W. Wu, T. J. Sanborn, K. Huang, R. N. Zuckermann and A. Barron (2001). Peptoid oligomers with a-chiral, aromatic side chains: Sequence requirements for the formation of stable peptoid helices. Journal of the American Chemical Society *123*, 6778-6784.

26. D. Y. Takamoto, M. M. Lipp, A. v. Nahmen, K. Y. C. Lee, A. J. Waring and J. A. Zasadzinski (2001). Interaction of lung surfactant proteins with anionic phospholipids. Biophysical Journal *81*, 153-169.

27. E. P. Ingenito, L. M. J. Morris, F. F. Espinosa, R. D. Kamm and M. Johnson (1999). Biophysical characterization and modeling of lung surfactant components. Journal of Applied Physiology *86*, 1702-1714.

28. R. N. Zuckermann, J. M. Kerr, S. B. H. Kent and W. H. Moos (1992). Efficient method for the preparation of peptoids [oligo(N-substituted glycines)] by submonomer solid-phase synthesis. J. Am. Chem. Soc. *114*, 10646-7.

29. A. P. Krapcho and C. S. Kuell (1990). Mono-Protected Diamines - N-Tert-Butoxycarbonyl-Alpha,Omega- Alkanediamines from Alpha,Omega-Alkanediamines. Synthetic Communications *20*, 2559-2564.

30. Y. Tanaka, T. Takei, T. Aiba, K. Masuda, A. Kiuchi and T. Fujiwara (1986). Development of synthetic lung surfactants. Journal of Lipid Research *27*, 475-485.

31. G. Putz, J. Goerke, H. W. Taeusch and J. A. Clements (1994). Comparison of captive and pulsating bubble surfactometers with use of lung surfactants. Journal of Applied Physiology *76*, 1425-1431.

**Figure Legends**

**Figure 1:** Mimic sequences.

Sequences of SP-$B_{1-25}$ peptide and peptoid mimics.

**Figure 2:** CD spectra

CD Spectra for SP-$B_{1-25}$ (circles), **1** (diamonds), and **2** (squares) in water (A) and liposomes (B).

**Figure 3:** LWSB isotherms.

LWSB isotherms for lipids alone (line), lipids + 2.16 mol% SP-$B_{1-25}$ (circles), lipids + 2.16 mol% **1** (diamonds), and lipids + 2.16 mol% **2** (squares) on buffer at 25°C with a barrier speed of 30 mm/min.

**Figure 4:** FM images.

FM images for lipids alone (A and E), lipids + 2.16 mol% SP-$B_{1-25}$ (B and F), lipids + 2.16 mol% **1** (C and G), and lipids + 2.16 mol% **2** (D and H) on buffer at 37°C with a barrier speed of 2-10 mm/min. Images shown for ~30 mN/m (A-D) and ~45 mN/m (E-H).

**Figure 5:** PBS static and dynamic adsorption data.

PBS static (A) and dynamic (B) adsorption data for lipids alone (line), lipids + 2.16 mol% SP-$B_{1-25}$ (circles), lipids + 2.16 mol% **1** (diamonds), and lipids + 2.16 mol% **2** (squares) in buffer at 37°C with a pulsation rate of 20 cycles/min.

**Figure 1**

SP-$B_{1-25}$ (Cys-Ala substitution):
$H_2N$-FPIPLPYAWLARALIKRIQAMIPKG-COOH

Peptoid **1**:
H-*N*spe-*N*spe-(*N*Lys-*N*spe-*N*spe)$_5$-$NH_2$

Peptoid **2**:
H-*N*ssb-*N*spe-(*N*Lys-*N*ssb-*N*spe)$_5$-$NH_2$

Peptoid **3**:
H-*N*ssb-*N*ssb-(*N*Lys-*N*ssb-*N*ssb)$_5$-$NH_2$

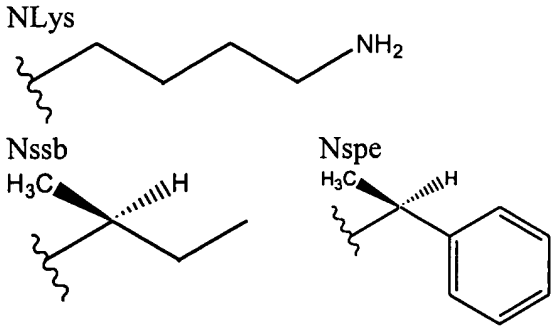

**Figure 2**

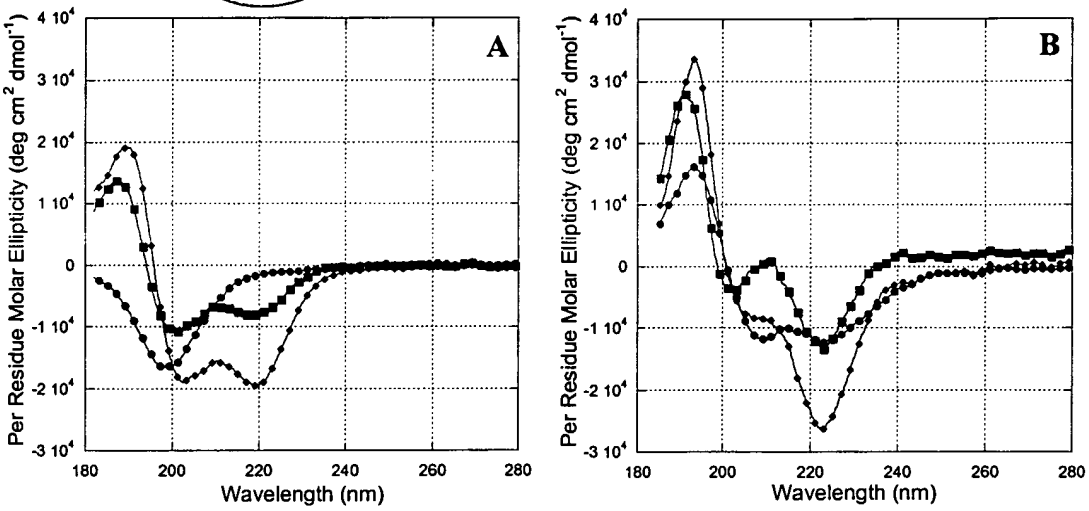

**Figure 3**

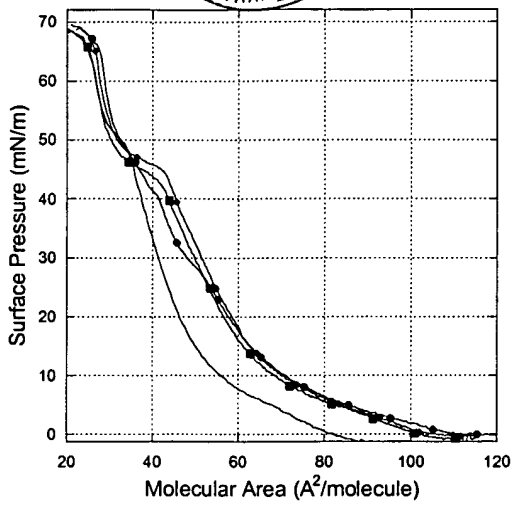

Figure 4

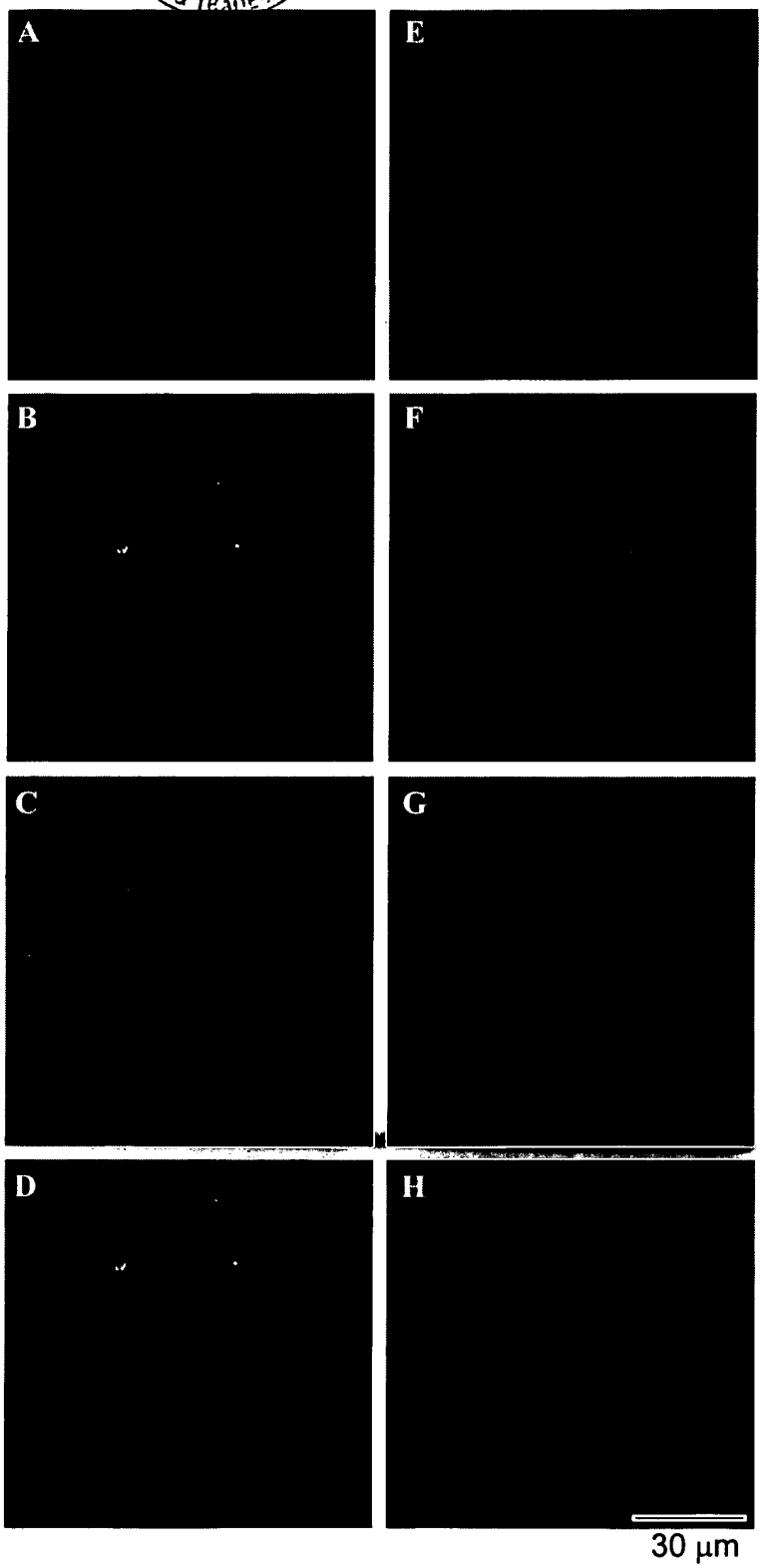

**Figure 5**